

# Myotubular myopathy and the neuromuscular junction: a novel therapeutic approach from mouse models

James J. Dowling<sup>1,\*‡</sup>, Romain Joubert<sup>2</sup>, Sean E. Low<sup>1</sup>, Ashley N. Durban<sup>3</sup>, Nadia Messaddeq<sup>4</sup>, Xingli Li<sup>1</sup>, Ashley N. Dulin-Smith<sup>3</sup>, Andrew D. Snyder<sup>3</sup>, Morgan L. Marshall<sup>3</sup>, Jordan T. Marshall<sup>3</sup>, Alan H. Beggs<sup>5</sup>, Anna Buj-Bello<sup>2,\*‡</sup> and Christopher R. Pierson<sup>3,\*‡</sup>

## SUMMARY

Myotubular myopathy (MTM) is a severe congenital muscle disease characterized by profound weakness, early respiratory failure and premature lethality. MTM is defined by muscle biopsy findings that include centralized nuclei and disorganization of perinuclear organelles. No treatments currently exist for MTM. We hypothesized that aberrant neuromuscular junction (NMJ) transmission is an important and potentially treatable aspect of the disease pathogenesis. We tested this hypothesis in two murine models of MTM. In both models we uncovered evidence of a disorder of NMJ transmission: fatigable weakness, improved strength with neostigmine, and electrodecrement with repetitive nerve stimulation. Histopathological analysis revealed abnormalities in the organization, appearance and size of individual NMJs, abnormalities that correlated with changes in acetylcholine receptor gene expression and subcellular localization. We additionally determined the ability of pyridostigmine, an acetylcholinesterase inhibitor, to ameliorate aspects of the behavioral phenotype related to NMJ dysfunction. Pyridostigmine treatment resulted in significant improvement in fatigable weakness and treadmill endurance. In all, these results describe a newly identified pathological abnormality in MTM, and uncover a potential disease-modifying therapy for this devastating disorder.

## INTRODUCTION

Myotubular myopathy (MTM), an X-linked congenital myopathy, is among the most severe childhood neuromuscular disorders (Jungbluth et al., 2008). Affected boys usually present in infancy with hypotonia, weakness and respiratory failure, and nearly half die in the first year of life (Herman et al., 2002; McEntagart et al., 2002). Those who survive have substantial disability, most often never achieving independent ambulation and usually requiring continuous ventilator support, and suffer premature lethality. There are no known treatments or disease-modifying therapies for this devastating disorder (Das et al., 1993).

MTM is the most common subtype of a larger group of childhood muscle diseases called centronuclear myopathies (CNMs) (Jungbluth et al., 2008). CNMs as a group are united by common features on muscle biopsy, including prominent centrally located nuclei, type I fiber predominance and hypotrophy, and irregular staining with oxidative enzymes (Pierson et al., 2005). Recent studies

also suggest that there are common pathomechanisms shared between subtypes of CNMs. Currently, mutations in four genes are associated with CNM: dynamin-2 (*DNM2*) (Bitoun et al., 2005), bridging integrator 1 (*BINI*) (Nicot et al., 2007), the skeletal muscle ryanodine receptor (*RYR1*) (Wilmshurst et al., 2010) and myotubularin (*MTM1*) (Laporte et al., 1996).

The only identified cause of MTM is mutation in *MTM1* (Das et al., 1993; Laporte et al., 1996; Herman et al., 2002). Myotubularin is a phosphoinositide phosphatase that regulates vesicle sorting within and through endosomal compartments (Robinson and Dixon, 2006; Cao et al., 2008; Dowling et al., 2008). Advances in our knowledge of myotubularin function and MTM disease pathogenesis have been greatly accelerated by the establishment of vertebrate models of the disease. In particular, recent work from several groups has identified a role for myotubularin in skeletal muscle in the formation and maintenance of the triad, the structure responsible for mediating excitation-contraction coupling (Al-Qusairi et al., 2009; Dowling et al., 2009; Al-Qusairi and Laporte, 2011). Additional studies on CNMs caused by *BINI*, *RYR1* and *DNM2* mutations have also documented structural and/or functional abnormalities in the triad (Al-Qusairi and Laporte, 2011; Toussaint et al., 2011). On the basis of these data, an emerging theory concerning MTM specifically, and CNMs in general, is that a primary mechanism of disease is abnormal  $Ca^{2+}$  homeostasis and impaired excitation-contraction coupling.

Myotubularin probably also performs additional functions within skeletal muscle that contribute to the disease phenotype. For example, a direct interaction between myotubularin and desmin was recently established, and examination of this interaction revealed that myotubularin might regulate the intracellular architecture and mitochondrial homeostasis within the myofiber (Hnia et al., 2011). Using a zebrafish model of MTM, we recently demonstrated that *mtm1* knockdown disturbs neuromuscular junction (NMJ) organization and that exposure to an

<sup>1</sup>Department of Pediatrics, Taubman Medical Research Institute, University of Michigan Medical Center, Ann Arbor, MI 48109-2200, USA

<sup>2</sup>Généthon, INSERM, Evry, France

<sup>3</sup>Research Institute, Nationwide Children's Hospital and Department of Pathology, Ohio State University College of Medicine, Columbus, OH, USA

<sup>4</sup>Imaging Center-Electron Microscopy, Institut de Génétique et de Biologie Moléculaire et Cellulaire, Illkirch, France

<sup>5</sup>Division of Genetics and Program in Genomics, The Manton Center for Orphan Disease Research, Children's Hospital Boston, Harvard Medical School, Boston, MA, USA

\*Authors for correspondence (jamedowl@umich.edu; abujbello@genethon.fr; Christopher.Pierson@nationwidechildrens.org)

‡These authors contributed equally to this work

Received 27 February 2012; Accepted 29 March 2012

© 2012. Published by The Company of Biologists Ltd  
This is an Open Access article distributed under the terms of the Creative Commons Attribution Non-Commercial Share Alike License (<http://creativecommons.org/licenses/by-nc-sa/3.0>), which permits unrestricted non-commercial use, distribution and reproduction in any medium provided that the original work is properly cited and all further distributions of the work or adaptation are subject to the same Creative Commons License terms.

acetylcholinesterase inhibitor improves motor function in morphant embryos (Robb et al., 2011). There is also evidence from previous ultrastructural examination of skeletal muscle from single cases of CNM or MTM for abnormalities in NMJ structure (Ambler et al., 1984; Fidzianska and Goebel, 1994; Liewluck et al., 2011). On the basis of these results, as well as the established link between endosomes and the regulation of NMJs (Bruneau and Akaaboune, 2006), we hypothesized that NMJ abnormalities (1) could be an additional contributing factor in MTM disease pathogenesis and (2) could be subject to modification via drug treatment.

To test these hypotheses, we used two existing murine models of MTM. The first, a gene knockout (KO) of myotubularin (*Mtm1*), has a severe phenotype, with onset of motor pathology at 2-4 weeks of age and death between 2-3 months of age (Buj-Bello et al., 2002). The second, a gene knock-in (KI) of a missense mutation (p.R69C) associated with mild clinical symptoms in individuals with MTM (Pierson et al., 2007), displays motor dysfunction starting at 3 months of age and death at approximately 12 months (Pierson et al., 2012). Both models exhibit the classic histopathological features observed in the skeletal muscles of individuals with MTM. In this study, using behavioral, neurodiagnostic and histopathological evaluations, we demonstrate that MTM mouse models have the characteristic features of dysfunction at the NMJ. Furthermore, using a randomized placebo-controlled study, we determine that treatment with the acetylcholinesterase inhibitor pyridostigmine improves MTM KI mouse motor function. In all, we describe a new aspect of pathogenesis in MTM and identify a promising therapy for this currently untreatable disease.

## RESULTS

### MTM mice have phenotypic and neurodiagnostic features of a disorder of NMJ transmission

We evaluated these models for evidence of a clinical disorder of NMJ transmission. In humans, disorders of the NMJ are characterized by exercise intolerance and fatigable weakness (Keesey, 2004). We examined these parameters in KI mice and their wild-type (WT) littermates. Exercise tolerance was measured by testing the ability of the mice to remain on a treadmill set at low speed (8 m/minute). As expected, all WT mice were able to walk for at least 25 minutes without difficulties. By contrast, KI mice could only tolerate an average of 8 minutes before stopping (Fig. 1A). Fatigable weakness was determined by measuring force generation during a series of repetitive forelimb grip measurements using a dynamometer (Fig. 1B). WT mice displayed no change in strength between grip 1 and grip 20, whereas KI mice exhibited a 40.1% decline in force generation. KI mice thus demonstrate both exercise intolerance and fatigable weakness. Of note, KO mice were too weak to tolerate these tests.

Two neurodiagnostic studies of NMJ dysfunction have been established in mouse models of a human NMJ disorder called myasthenia gravis (Wu et al., 2001). The first is a pharmacological test whereby strength is measured before and after administration of a short-acting acetylcholinesterase inhibitor. We performed this test by measuring grip strength before and after neostigmine infusion. WT mice had no change in force generation with drug treatment. By contrast, KI mice experienced a 116% increase in grip strength after neostigmine administration ( $n=12$ ,  $P<0.001$ ). The second study is a repetitive stimulation nerve conduction study,

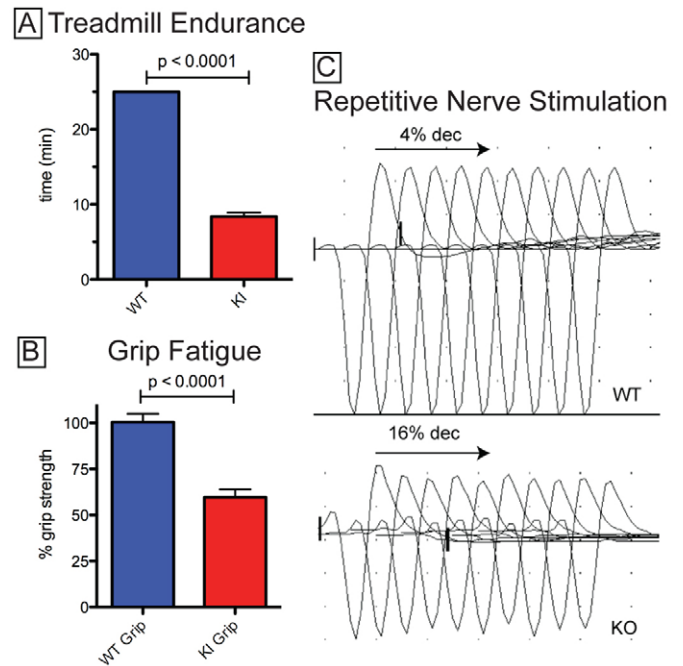


**Fig. 1. MTM mice have a disorder of NMJ transmission.** (A) 5-month-old KI mice and WT littermates were placed on a treadmill at 8 m/minute. All WT mice remained on for 25 minutes, whereas KI mice remained on for only  $8.4 \pm 0.5$  minutes ( $n=5$ ,  $P<0.0001$ ). (B) Grip fatigue was assayed by measuring forelimb force generation over 20 consecutive grips. Data are expressed as the % strength difference between grips 20 and 1. For WT animals, grip 20 was  $100.4 \pm 4.6\%$  the value of grip 1. For KI animals, grip 20 was  $59.9 \pm 4.3\%$  the value of grip 1 ( $n=5$  animals,  $P<0.0001$ ). Of note, KO mice were too weak to tolerate either the treadmill or the grip fatigue tests. (C) Compound motor action potentials (CMAPs) recorded from gastrocnemius with 3-Hz repetitive nerve stimulation at the sciatic notch. Depicted are CMAPs from a train of ten stimuli. % decrement (dec) was determined by comparing the CMAP amplitudes of the first and fifth peaks. In these traces, WT CMAP exhibited a 4% decrement, whereas KO CMAP showed a 16% decrement.

which is a diagnostic gold standard in individuals with NMJ disorders. A positive result is indicated by a decremental response of 10% or greater in the amplitude of compound muscle action potentials with 3-Hz repetitive stimulation. All control mice tested had a normal response (i.e. no decrement  $>10\%$ ). Conversely, 2/5 of KI mice and 12/18 KO mice had a positive test ( $\geq 10\%$  decrement), with an average decrement in KO mice of  $11.5 \pm 1.5\%$ , compared with an average value of  $2.0 \pm 0.9\%$  for WT ( $P=0.0002$ ). Sample studies from a control and a KO mouse are shown in Fig. 1C. In combination with the 'clinical' assessment, both diagnostic tests strongly support the presence of an NMJ defect in MTM mouse models.

### MTM mouse models exhibit histopathological abnormalities at the NMJ

To better understand the basis of the NMJ phenotype that is present in MTM mice, we performed a histopathological analysis of junctions in WT and *Mtm1* KO animals. We first imaged NMJs in situ in skeletal muscle using fluorescently conjugated  $\alpha$ -bungarotoxin to label acetylcholine receptors (AChRs) (Fig. 2). In

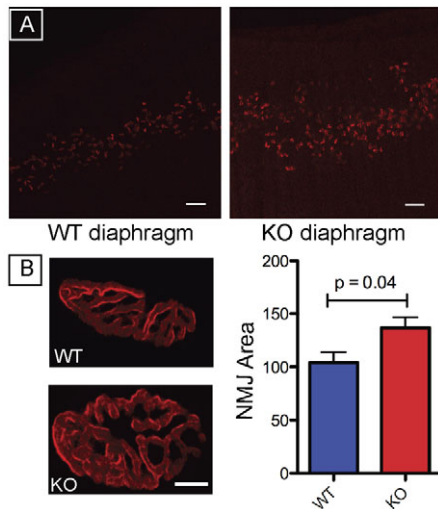


**Fig. 2. NMJ abnormalities in MTM KO mice.** (A)  $\alpha$ -bungarotoxin–Alexa-Fluor-594 staining of isolated whole-mount diaphragm muscle from 5-week-old WT and MTM KO mice. WT diaphragms show a discrete, concentrated band of staining, whereas KO mice had a more diffuse and less organized pattern of staining. Scale bars: 110  $\mu$ m. (B) Confocal image of  $\alpha$ -bungarotoxin staining from an isolated tibialis anterior myofiber from 5-week-old WT and KO mice. Individual junctions from KOs have a similar overall appearance to those from WT but are significantly larger. Scale bar: 20  $\mu$ m. Right panel: quantification of the overall area of NMJs as determined from images similar to that on the left. Values (in arbitrary units) were 104.0 $\pm$ 9.9 (WT) vs 136.7 $\pm$ 10.1 (KO) ( $n$ =30 junctions,  $P$ =0.04).

WT mice, staining of whole diaphragm demonstrated a tight band of receptors in the center of the tissue. Conversely, staining of diaphragm in KO mice revealed a dispersed and disorganized band of AChRs (Fig. 2A). We quantified this difference by measuring the maximum width of  $\alpha$ -bungarotoxin staining in each sample. KO mice had a significantly greater width of staining as compared with controls (0.37 $\pm$ 0.01 vs 0.86 $\pm$ 0.03,  $n$ =5,  $P$ <0.0001).

We next analyzed individual junctions by staining isolated myofibers with  $\alpha$ -bungarotoxin. Junctions from KO animals retained a normal overall appearance of staining, but were substantially larger than junctions from WT animals (Fig. 2B). We performed a similar analysis in KI mice, and found that NMJs were 30% larger than in age-matched littermates ( $n$ =30,  $P$ =0.01).

We lastly examined NMJ ultrastructure using electron microscopy (Fig. 3). Muscle from WT mice exhibited dense, membranous areas with deep and complex invaginations that are typical of murine NMJs. Muscle from KO animals, conversely, contained NMJs with multiple abnormalities, including severe simplification of the post-synaptic junctional appearance with shallower and less complex invaginations. In addition, the subjunctional sarcoplasm appeared disorganized and contained many vacuolar structures. Of note, the density along the immediate postsynaptic membrane appeared qualitatively similar to that of WT junctions, in keeping with the light microscopic findings with  $\alpha$ -bungarotoxin. In all, MTM mice have structurally abnormal NMJs, exhibiting both increased size as well as reduced complexity.

### Altered neuregulin signaling as a mechanism underlying NMJ size changes in MTM mice

We then investigated potential pathomechanisms for the observed structural changes in NMJs from MTM mice. To determine whether the increase in junction size correlated with changes in gene expression, expression levels of components of the NMJ were examined by quantitative reverse-transcriptase PCR (qRT-PCR). Consistent with our histochemical data, expression of several NMJ-associated transcripts (*AchE*, *Chrna*, *Chrnng*, *Chrnd*, *Chrme* and *MuSK*) was increased in both KO and KI muscle (Fig. 4A). These changes were detected at early phenotypic stages and were maintained in older animals as well. Neuregulin (*Nrg1*) gene expression was also increased; this observation, in combination with increased AChR subunit expression, is suggestive of upregulation of the neuregulin (NRG) signaling pathway (Rimer, 2007). Consequently, the NRG pathway was evaluated by measuring ERK phosphorylation, a known downstream modification of NRG

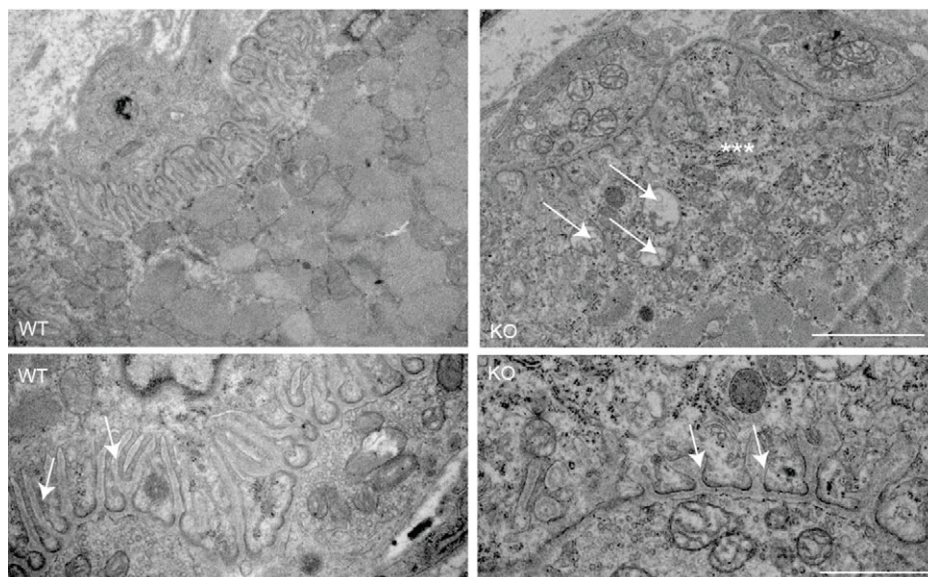


**Fig. 3. Ultrastructural abnormalities in the NMJs of MTM KO mice.** Ultrastructural examination of NMJs from the tibialis anterior muscle from 4-week-old WT and KO mice. Low-magnification images (top panels) illustrate the presence of vacuoles (arrows) and disorganized, amorphous material in the subjunctional space (\*\*\*) in KO mice. Scale bar: 2  $\mu$ m. High-magnification images (bottom panels) reveal simplification of the post junctional folds (arrows) in KO mice. Scale bar: 1  $\mu$ m.

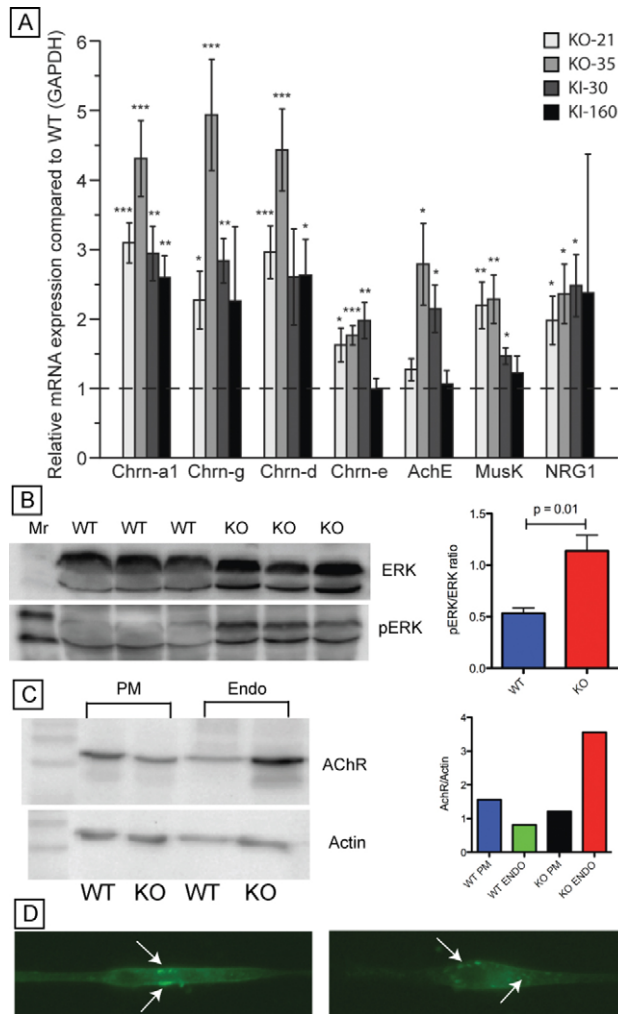


**Fig. 4. Alterations in gene expression and AChR localization in MTM KO mice.** (A) Gene expression analysis of components of the NMJ using qRT-PCR. RNA was pooled from quadriceps muscle from 21- and 35-day-old KO and 30- and 160-day-old KIs. All values are normalized with GAPDH and then expressed as a fold comparison with age-matched WT littermate values. Significant increases were observed in both young and old KO and KI animals for several components of the NMJ as well as for neuregulin (NRG1). The relative mRNA levels of *AchE*, *Chrna1*, *Chrn-g*, *Chrn-d*, *Chrne*, *MusK* and *Nrg1* from quadriceps of 21 ( $n=9$ )- or 35 ( $n=8$ )-day-old *Mtm1* KO mice and 30 ( $n=5$ )- or 160 ( $n=5$ )-day-old *Mtm1* KI mice were quantified by qRT-PCR, normalized to GAPDH expression, and compared with WT levels. \* $P<0.05$ ; \*\* $P<0.01$ ; \*\*\* $P<0.001$  (vs WT). (B) Western blot analysis of protein extracts from 5-week-old WT and KO quadriceps muscle using antibodies to ERK and pERK. Right panel shows quantification of bands by densitometry. Values (pERK:ERK) were  $0.53\pm 0.05$  (WT) and  $1.14\pm 0.15$  (KO) ( $n=3$ ,  $P=0.01$ ). Mr, molecular weight. (C) Western blot analysis of protein extracts from myotubes differentiated from pools of myoblasts isolated from 4-week-old WT and KO animals. Blots were probed with antibodies to AChR, actin and Rab5 [an endosomal marker used to verify successful fractionation of endosomes (Endo) from plasma membrane (PM) (data not shown)]. Quantification of bands from the blot are shown in the right panel. Data represent the ratio of AChR:actin for each subcellular fraction. Actual values were as follows: 1.56 (WT PM), 0.81 (WT ENDO), 1.21 (KO PM) and 3.56 (KO ENDO). (D)  $\alpha$ -bungarotoxin labeling of differentiated myotubes. Cells were incubated in Alexa-Fluor-488-conjugated  $\alpha$ -bungarotoxin (Invitrogen) for 45 minutes and then either immediately imaged or else imaged 45 minutes or 4 hours after removal of the  $\alpha$ -bungarotoxin. Images shown are from 4 hours after removal of  $\alpha$ -bungarotoxin. In WT myotubes (left panel), labeling is found along the outer membrane surface, whereas, in KO myotubes (right panel), the staining is detected in puncta within the cytoplasm (arrows) ( $n=10$  per condition).

signaling (Won et al., 1999). Consistent with increased NRG signaling, phosphorylated ERK (pERK) levels were significantly increased in KO mice as compared with WT littermates (Fig. 4B).

#### Abnormal membrane traffic as a mechanism underlying NMJ structural changes in MTM mice

Changes in gene expression and abnormal pERK levels probably do not account for the ultrastructural changes in the NMJs. Given the simplified, vacuolated appearance of the junctions, one possible explanation is aberrant regulation of junctional membrane turnover. To test for this, protein extracts from differentiated myotubes were fractionated to measure the levels of AChR at the plasma membrane and within the internalized endosomal fraction. A significant increase in the overall amount and ratio of AChRs associated with the endosomal fraction was detected in KO myotubes (Fig. 4C). AChR recycling was further studied by examining receptor internalization in differentiated myotubes after a pulsed exposure to fluorescently conjugated  $\alpha$ -bungarotoxin. After a 1-hour pulse, there was no difference in  $\alpha$ -bungarotoxin staining. By contrast, after a 4-hour chase, there was a visible increase in the number of  $\alpha$ -bungarotoxin puncta within *Mtm1* KO myotubes, consistent with

a failure of export from the endosomal fraction (Fig. 4D). In combination, these data suggest abnormal NMJ trafficking as one potential explanation for the observed ultrastructural abnormalities. These data are also consistent with our observation of mislocalized and disorganized NMJs as seen with examination of muscle in situ (Fig. 2A).

#### Treatment with pyridostigmine improves the motor phenotype in MTM KI mice

Treatment with acetylcholinesterase inhibitors is beneficial in individuals with primary diseases of the NMJ (Abicht and Lochmuller, 1993; Skeie et al., 2010). We thus hypothesized that such treatment should improve aspects of the motor phenotype in MTM mice as well. To test this, we performed a randomized trial involving pyridostigmine, an acetylcholinesterase inhibitor widely used in humans (Maggi and Mantegazza, 2011). Starting at 5 months of age, KI animals were given intraperitoneal (IP) injections of either phosphate-buffered saline (PBS) or pyridostigmine four times daily for a total of 4 weeks. Animals were tested for grip fatigue and treadmill endurance immediately prior to initiation of the trial, at 2 and 4 weeks of treatment, and 2 weeks after treatment was discontinued. No statistical difference was seen in either measure prior to treatment. PBS-treated animals experienced an increase in grip fatigue and a decline in treadmill endurance during the 4-week period of the drug trial. Conversely, pyridostigmine-treated animals showed a modest improvement in grip fatigue and a substantial change in treadmill endurance at all time points examined. Both measures were statistically significantly improved

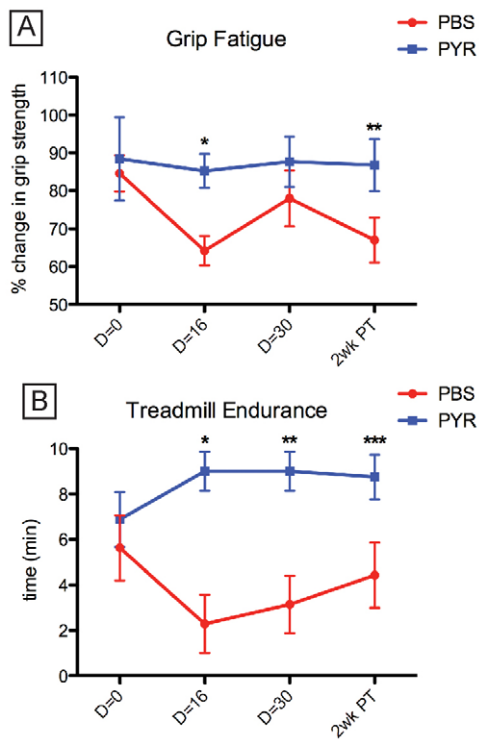


**Fig. 5. Pyridostigmine treatment improves motor function in MTM KI animals.** KI animals were treated with either PBS or pyridostigmine (PYR) four times daily for 30 days (n=8 per condition). Measurements were made at the initiation of the trial, 16 and 30 days into the trial (D=16 and D=30), and 2 weeks after conclusion of the trial (2wk PT). Examiners were blinded to experimental condition. Measurements were recorded as per Fig. 1. (A) There was significant reduction in grip fatigue with PYR treatment. This improvement reached statistical significance at day 16 and 2 weeks post treatment, and was suggestive but not significant at day 30. Data are expressed as the percentage of grip 20/grip 1. For PBS, results were: 84.5±4.8% (D=0), 64.2±3.9% (D=16), 78.0±7.3% (D=30) and 67.0±5.9% (2wk PT). For PYR, results were: 88.4±11.0% (D=0; n.s. vs PBS D=0), 85.2±4.5% (D=16; \*P=0.001 vs PBS D=16), 87.7±6.6% (D=30; P=0.17 vs PBS D=30) and 86.8±6.9% (2wk PT; \*\*P=0.02 vs PBS 2wk PT). (B) Treatment with PYR significantly improved treadmill endurance at all times tested. For PBS treatment, times were (in minutes): 5.6±1.4 (D=0), 2.3±1.3 (D=16), 3.1±1.3 (D=30) and 4.4±1.4 (2wk PT). For PYR treatment, times were: 6.9±1.2 (D=0; n.s. vs PBS D=0), 9.0±0.9 (D=16; \*P=0.0003 vs PBS D=16), 9.0±0.9 (D=30; \*\*P=0.002 vs PBS D=30) and 8.8±1.0 (2wk PT; \*\*\*P=0.02 vs PBS 2wk PT).

as compared with PBS-treated littermates (Fig. 5). Of note, these improvements persisted beyond the conclusion of the trial.

## DISCUSSION

In summary, we demonstrate that (1) MTM mice have features of a clinical disorder of NMJ transmission, (2) these clinical changes are correlated with structural changes in the NMJ, and (3) pyridostigmine, an acetylcholinesterase inhibitor, improves aspects of the MTM mouse motor phenotype. These results are important because they identify a previously unknown aspect of MTM disease pathogenesis and provide preclinical evidence (in the form of a placebo-controlled study) for the first potential therapy for this devastating disease.

Additional support for the presence of NMJ pathology in MTM and for the potential efficacy of pyridostigmine comes from two recent case studies. The first study reported four individuals (one with MTM and three with genetically undefined CNMs) with the clinical and electrodiagnostic features of a disorder of NMJ transmission (Robb et al., 2011). All four individuals had at least some positive benefit when treated with pyridostigmine, with one individual regaining ambulation after starting medication. The second study documented a single case of CNM (genetic cause unknown) with features of an NMJ disorder and a positive response to pyridostigmine (Liewluck et al., 2011). This case additionally included ultrastructural analysis that revealed simplified postsynaptic regions that were similar in appearance to the MTM KO mice (Fig. 4). Similar findings were reported in a case of MTM (without genetic confirmation) (Ambler et al., 1984; Fidzińska and Goebel, 1994; Liewluck et al., 2011). These results support the consideration of pyridostigmine (or other modulators of NMJ function) for the treatment of individuals with MTM, and also suggest that NMJ pathology might be a shared feature of all CNMs.

An important issue raised by this study is the nature of the pathomechanisms responsible for NMJ pathology in the setting of myotubularin mutation. The NMJs in the mouse models are both larger and greatly simplified in ultrastructure compared with WT. Our data support a hypothesis whereby the increased junctional size is due to abnormal NRG signaling and the aberrant junctional structure is caused by defective AChR trafficking. Given that myotubularin is a known regulator of endosomal dynamics (Dowling et al., 2008; Nicot and Laporte, 2008), and that both AChR trafficking and NRG signaling are dependent on endocytic machinery (Bruneau et al., 2005; Yang et al., 2005; Bruneau and Akaaboune, 2006), this hypothesis plausibly fits with the loss of myotubularin function. At present, the abnormalities in receptor recycling do not completely explain the ultrastructural changes observed on electron microscopy. Other factors are likely to contribute, including changes induced by muscle inactivity and the potential role of dysregulated Ca<sup>2+</sup> homeostasis. Also, given the fact that knockout of desmin in mice also causes NMJ abnormalities (including disorganization and simplification of the junctions) (Agbulut et al., 2001), it is possible that some of the NMJ abnormalities in the MTM KO mice result from the loss of the recently described desmin-myotubularin interactions (Hnia et al., 2011). Future experimentation will be required to better test these concepts and to further delineate the mechanism(s) of pathology.

The need for therapy development for MTM is crucial. Approximately 50% of boys with MTM die in the first year of life, and those that survive have substantial disability in the form of chronic ventilator dependence and impaired ambulation (Das et al., 1993; Herman et al., 2002; McEntagart et al., 2002). Although pyridostigmine is not expected to be a curative therapy, the possibility that it could improve motor function in patients and thus positively alter disease course makes it an extremely attractive therapeutic candidate. This is especially true given that pyridostigmine is routinely used in children and adults without significant adverse effects (Skeie et al., 2010; Maggi and Mantegazza, 2011). In addition, pyridostigmine is unlikely to interfere with additional therapeutic strategies being considered for MTM [such as, for example, myostatin inhibition (Lawlor et

al., 2011) or gene therapy (Buj-Bello et al., 2008)], and thus would make a useful adjunct treatment strategy. In the future, it will be important to compare the effect of pyridostigmine with 3,4-DAP (diaminopyridine), a drug that promotes the release of acetylcholine from presynaptic nerve termini and has been effective in Lambert-Eaton syndrome (Wirtz et al., 2010) and in some cases of congenital myasthenic syndrome (Kinali et al., 2008). It is possible that 3,4-DAP is equally or more effective than pyridostigmine, and that the two drugs in combination could synergistically improve motor function.

In conclusion, using murine models of MTM, we have identified a previously unknown disease pathomechanism and a potential therapy based on this observation. On the basis of the results presented in this study, along with case reports supporting an NMJ phenotype in individuals with CNM, we propose that pyridostigmine would make an excellent therapeutic candidate to be tested in the clinical trial setting.

## METHODS

### Mice

*Mtm1* KO and KI mice have been described previously (Buj-Bello et al., 2002; Pierson et al., 2012) and were maintained on a C56BL6 background (129PAS background for qRT-PCR) according to IUCUC guidelines at the various institutions (University of Michigan, Nationwide Children's Hospital and Genethon). All studies were conducted on hemizygous affected male animals carrying the indicated mutations and age-matched male WT littermates.

### Grip fatigue testing

Grip fatigue testing was performed as described previously (Miller et al., 2006). Force generated after treadmill walking from each of 20 consecutive grip strength measurements was determined using a dynamometer (Columbus Instruments). Grip fatigue was calculated as the percent difference in force between the twentieth and the first grip.

### Neostigmine challenge

Neostigmine challenge was performed as described previously (Wu et al., 2001). Grip strength was measured as above, and then a neostigmine bromide dose of 0.75  $\mu$ g was administered with 0.3  $\mu$ g atropine sulfate (both from Sigma) mixed in PBS and injected IP in 50  $\mu$ l total volume. Five minutes later, grip strength was measured as above.

### Repetitive nerve stimulation testing

Repetitive nerve stimulation testing was performed as described previously (Wu et al., 2001). Animals were anesthetized with ketamine. A stimulating electrode was placed at the sciatic notch and a recording electrode was placed in the corresponding gastrocnemius muscle. First, a single super-maximal stimulation was given to verify the ability to detect a compound muscle action potential (CMAP). Then, a train of stimuli at 3 Hz was applied and the resulting CMAPs recorded using a Viking nerve conduction recording system.

### Pyridostigmine trial

Following a baseline [Day (D)=0] determination of grip strength fatigue and treadmill endurance, 0.1  $\mu$ g/g of pyridostigmine was administered four times a day to 5-month-old KI mice for 30 days. Grip strength fatigue and treadmill endurance were determined 16 (D=16) and 30 (D=30) days after the initiation of treatment and 2 weeks post-treatment, when pyridostigmine injections were completed. PBS alone was injected as a control. Personnel performing the injections and all testing were blinded to the agent injected.

### $\alpha$ -bungarotoxin labeling whole diaphragms

This was performed as described previously (Mejat et al., 2009). Five-week-old mice were euthanized and diaphragms were isolated by dissection. They were then fixed briefly in 2% paraformaldehyde and incubated overnight with  $\alpha$ -bungarotoxin conjugated to Alexa Fluor 594 (Invitrogen) diluted 1:1000. Samples were mounted with ProLong gold (Invitrogen) and then viewed using an Olympus confocal microscope.

### $\alpha$ -bungarotoxin labeling of isolated myofibers

This was performed as described previously (Mejat et al., 2009). Mice were euthanized by cervical dislocation and then tibialis anterior muscles were isolated and fixed briefly in 2% paraformaldehyde. Whole muscles were stained with  $\alpha$ -bungarotoxin as above, and staining was visualized using a Zeiss LSM 510-Meta confocal microscope.

### Electron microscopy

Electron microscopy was performed as previously described (Buj-Bello et al., 2002).

### qRT-PCR

Real time PCR was performed using an ABI Prism 7900 apparatus (Applied Biosystems). Primers are listed below in Table 1.

**Table 1. Oligonucleotide primer sequences for qRT-PCR**

Primer	Forward (5'-3')	Reverse (5'-3')
AchE	AAGGGCTGGGATATAATACGAC	CTTAGCCCAAGACATGCAGA
Chrna1	GAATCCAGATGACTATGGAG	GACAATGATCTCACAGTAGC
Chrng	ATCCGGCACCGACCGCTAA	CATTTCTGCCCGCCGCTT
Chrnd	AACGTGTGGATAGATCATGC	CATAGACAAGCACATTGCAGG
Chrne	AGACCTACAATGCTGAGGAGG	GGATGATGAGCGTATAGATGA
GAPDH	TTGTGATGGGTGTGAACAC	TTCAGTCTGGGATGACCTT
MuSK	CTCGTCTCCCATTAATGTAAAAA	TCCAGCTTCACCAGTTTGAGTAA
Nrg1	CCTGGGAGGCCCTCGCAAT	CCGTATGCTGGACACGGGT

AchE, acetylcholinesterase; Chrna1, cholinergic receptor nicotinic  $\alpha$ -1; Chrng, cholinergic receptor nicotinic  $\gamma$ ; Chrnd, cholinergic receptor nicotinic delta; Chrne, cholinergic receptor nicotinic epsilon; GAPDH, glyceraldehyde-3-phosphate dehydrogenase; MuSK, muscle skeletal receptor tyrosine kinase; Nrg1, neuregulin-1.

## TRANSLATIONAL IMPACT

### Clinical issue

Myotubular myopathy (MTM), which is one of several diseases collectively classified as centronuclear myopathies, is a devastating neuromuscular disease of childhood characterized by weakness, severe disability and, in most instances, early lethality. The genetic basis for the disease is known – mutation of the myotubularin (*MTM1*) gene – but this knowledge has not translated into the development of viable treatment strategies.

### Results

In this study, the authors tested the hypothesis that defective transmission at the neuromuscular junction (NMJ) is a pathological and treatable feature of MTM. Their characterization of two existing mouse models of MTM revealed signs consistent with an NMJ disorder, with pathological changes indicating a primary abnormality in the NMJ. Treatment of the mice with pyridostigmine, a known modulator of the NMJ, resulted in significant improvement in motor function.

### Implications and future directions

These data identify NMJ dysfunction as a previously unrecognized aspect of MTM pathology. No treatments currently exist for MTM, and these findings represent an important step towards translation of the first potential therapy. Pyridostigmine is already approved for other indications, and these preclinical data support initiation of a clinical trial to test the ability of this drug (or other drugs that modulate the NMJ) to improve disease in individuals with MTM. In addition, given the similarities between the pathology of MTM and other centronuclear myopathies, it is likely that NMJ abnormalities are a general and potentially treatable feature in all individuals affected by this group of diseases.

### Primary myocytes

Myocytes were derived from extensor digitorum longus muscles from 28-day-old KO animals and WT siblings per an established protocol (Rando and Blau, 1994). All experiments were performed on myotubes differentiated with 2% horse serum for 10-14 days.

### Western blot analysis on skeletal muscle

Total protein was extracted from quadriceps or primary myotubes using the T-PER reagent (Pierce). Western blots were performed as detailed previously (Dowling et al., 2009). The following antibodies were used: ERK or pERK (1:1000; Cell Signaling), AChR (1:1000; Covance), actin (1:3000; Cell Signaling) and Rab5 (1:500; Abcam). All secondary antibodies were used at 1:2000 (Santa Cruz Biotech).

### $\alpha$ -bungarotoxin recycling

See Kumari et al. for details (Kumari et al., 2008). Myotubes were incubated with Alexa-Fluor-488-conjugated  $\alpha$ -bungarotoxin for 45 minutes at room temperature, washed with media, and examined by live imaging 1 hour and 4 hours after  $\alpha$ -bungarotoxin exposure using a Leica inverted microscope.

### Statistical analyses

All statistical analyses were performed using GraphPad Prism. Data was from various studies was entered into the program and then analyzed using a Student's *t*-test.

### ACKNOWLEDGEMENTS

The authors acknowledge Karine Poulard for excellent technical expertise, John Hayes for assistance with neurodiagnostic studies, and Drs Eva Feldman and Henry Paulson for critical reading of the manuscript.

### COMPETING INTERESTS

The authors declare that they do not have any competing or financial interests.

### AUTHOR CONTRIBUTIONS

J.J.D., A.B.-B. and C.R.P. conceived the experimentation, interpreted the data and jointly wrote the manuscript. R.J. assisted with gene expression analysis, and N.M. with electron microscopy and interpretation of ultrastructure. S.E.L. and X.L. performed histopathological analyses and assisted in data interpretation. A.N.D., A.N.D.-S., A.D.S., M.L.M. and J.T.M. performed clinical assessments of the KI mice and helped carry out the drug screen. A.H.B. provided assistance with data interpretation and development of the manuscript.

### FUNDING

This study was funded primarily through research grants from the Muscular Dystrophy Association [MDA 186999 to J.J.D. and C.R.P.; MDA 201302 to A.H.B.; MDA 155638 to C.R.P.]; by the Taubman Medical Institute (J.J.D.); by the National Institutes of Health [NIH 1K08AR054835 to J.J.D.; NIH K08NS49095 to C.R.P.; R01AR044345 to A.H.B.]; by the Joshua Frase Foundation (A.H.B.); by the Lee and Penny Anderson Family Foundation (A.H.B.); by the Association Française contre les Myopathies (AFM) (A.B.-B.); by the Myotubular Trust (A.B.-B.); by the ATIGE-Genopole d'Evry, France (A.B.-B.).

### REFERENCES

- Abicht, A. and Lochmuller, H. (1993). Congenital Myasthenic Syndromes. In *Gene Reviews* (ed. R. A. Pagon, T. D. Bird, C. R. Dolan et al.). Seattle: University of Washington Press.
- Agbulut, O., Li, Z., Perie, S., Ludosky, M. A., Paulin, D., Cartaud, J. and Butler-Browne, G. (2001). Lack of desmin results in abortive muscle regeneration and modifications in synaptic structure. *Cell Motil. Cytoskeleton* **49**, 51-66.
- Al-Qusairi, L. and Laporte, J. (2011). T-tubule biogenesis and triad formation in skeletal muscle and implication in human diseases. *Skelet. Muscle* **1**, 26.
- Al-Qusairi, L., Weiss, N., Toussaint, A., Berbey, C., Messaddeq, N., Kretz, C., Sanoudou, D., Beggs, A. H., Allard, B., Mandel, J. L. et al. (2009). T-tubule disorganization and defective excitation-contraction coupling in muscle fibers lacking myotubularin lipid phosphatase. *Proc. Natl. Acad. Sci. USA* **106**, 18763-18768.
- Ambler, M. W., Neave, C. and Singer, D. B. (1984). X-linked recessive myotubular myopathy: II. Muscle morphology and human myogenesis. *Hum. Pathol.* **15**, 1107-1120.
- Bitoun, M., Maugendre, S., Jeannot, P. Y., Lacene, E., Ferrer, X., Laforet, P., Martin, J. J., Laporte, J., Lochmuller, H., Beggs, A. H. et al. (2005). Mutations in dynamin 2 cause dominant centronuclear myopathy. *Nat. Genet.* **37**, 1207-1209.
- Bruneau, E. G. and Akaaboune, M. (2006). Running to stand still: ionotropic receptor dynamics at central and peripheral synapses. *Mol. Neurobiol.* **34**, 137-151.
- Bruneau, E., Sutter, D., Hume, R. I. and Akaaboune, M. (2005). Identification of nicotinic acetylcholine receptor recycling and its role in maintaining receptor density at the neuromuscular junction in vivo. *J. Neurosci.* **25**, 9949-9959.
- Buj-Bello, A., Laugel, V., Messaddeq, N., Zahreddine, H., Laporte, J., Pellissier, J. F. and Mandel, J. L. (2002). The lipid phosphatase myotubularin is essential for skeletal muscle maintenance but not for myogenesis in mice. *Proc. Natl. Acad. Sci. USA* **99**, 15060-15065.
- Buj-Bello, A., Fougerousse, F., Schwab, Y., Messaddeq, N., Spohner, D., Pierson, C. R., Durand, M., Kretz, C., Danos, O., Douar, A. M. et al. (2008). AAV-mediated intramuscular delivery of myotubularin corrects the myotubular myopathy phenotype in targeted murine muscle and suggests a function in plasma membrane homeostasis. *Hum. Mol. Genet.* **17**, 2132-2143.
- Cao, C., Backer, J. M., Laporte, J., Bedrick, E. J. and Wandinger-Ness, A. (2008). Sequential actions of myotubularin lipid phosphatases regulate endosomal PI(3)P and growth factor receptor trafficking. *Mol. Biol. Cell* **19**, 3334-3346.
- Das, S., Dowling, J. and Pierson, C. R. (1993). X-linked centronuclear myopathy. In *Gene Reviews* (ed. R. A. Pagon, T. D. Bird, C. R. Dolan et al.). Seattle: University of Washington Press.
- Dowling, J. J., Gibbs, E. M. and Feldman, E. L. (2008). Membrane traffic and muscle: lessons from human disease. *Traffic* **9**, 1035-1043.
- Dowling, J. J., Vreede, A. P., Low, S. E., Gibbs, E. M., Kuwada, J. Y., Bonnemann, C. G. and Feldman, E. L. (2009). Loss of myotubularin function results in T-tubule disorganization in zebrafish and human myotubular myopathy. *PLoS Genet.* **5**, e1000372.
- Fidzianska, A. and Goebel, H. H. (1994). Aberrant arrested in maturation neuromuscular junctions in centronuclear myopathy. *J. Neurol. Sci.* **124**, 83-88.
- Herman, G. E., Kopacz, K., Zhao, W., Mills, P. L., Metznerberg, A. and Das, S. (2002). Characterization of mutations in fifty North American patients with X-linked myotubular myopathy. *Hum. Mutat.* **19**, 114-121.
- Hnia, K., Tronchere, H., Tomczak, K. K., Amoasii, L., Schultz, P., Beggs, A. H., Payastre, B., Mandel, J. L. and Laporte, J. (2011). Myotubularin controls desmin

- intermediate filament architecture and mitochondrial dynamics in human and mouse skeletal muscle. *J. Clin. Invest.* **121**, 70-85.
- Jungbluth, H., Wallgren-Pettersson, C. and Laporte, J.** (2008). Centronuclear (myotubular) myopathy. *Orphanet. J. Rare Dis.* **3**, 26.
- Keesey, J. C.** (2004). Clinical evaluation and management of myasthenia gravis. *Muscle Nerve* **29**, 484-505.
- Kinali, M., Beeson, D., Pitt, M. C., Jungbluth, H., Simonds, A. K., Aloysius, A., Cockerill, H., Davis, T., Palace, J., Manzur, A. Y. et al.** (2008). Congenital myasthenic syndromes in childhood: diagnostic and management challenges. *J. Neuroimmunol.* **201-202**, 6-12.
- Kumari, S., Borroni, V., Chaudhry, A., Chanda, B., Massol, R., Mayor, S. and Barrantes, F. J.** (2008). Nicotinic acetylcholine receptor is internalized via a Rac-dependent, dynamin-independent endocytic pathway. *J. Cell Biol.* **181**, 1179-1193.
- Laporte, J., Hu, L. J., Kretz, C., Mandel, J. L., Kioschis, P., Coy, J. F., Klauck, S. M., Poustka, A. and Dahl, N.** (1996). A gene mutated in X-linked myotubular myopathy defines a new putative tyrosine phosphatase family conserved in yeast. *Nat. Genet.* **13**, 175-182.
- Lawlor, M. W., Read, B. P., Edelstein, R., Yang, N., Pierson, C. R., Stein, M. J., Wermer-Colan, A., Buj-Bello, A., Lachey, J. L., Seehra, J. S. et al.** (2011). Inhibition of activin receptor type IIb increases strength and lifespan in myotubularin-deficient mice. *Am. J. Pathol.* **178**, 784-793.
- Liewluck, T., Shen, X. M., Milone, M. and Engel, A. G.** (2011). Endplate structure and parameters of neuromuscular transmission in sporadic centronuclear myopathy associated with myasthenia. *Neuromuscul. Disord.* **21**, 387-395.
- Maggi, L. and Mantegazza, R.** (2011). Treatment of myasthenia gravis: focus on pyridostigmine. *Clin. Drug. Investig.* **31**, 691-701.
- McEntagart, M., Parsons, G., Buj-Bello, A., Biancalana, V., Fenton, I., Little, M., Krawczak, M., Thomas, N., Herman, G., Clarke, A. et al.** (2002). Genotype-phenotype correlations in X-linked myotubular myopathy. *Neuromuscul. Disord.* **12**, 939-946.
- Mejat, A., Decostre, V., Li, J., Renou, L., Kesari, A., Hantai, D., Stewart, C. L., Xiao, X., Hoffman, E., Bonne, G. et al.** (2009). Lamin A/C-mediated neuromuscular junction defects in Emery-Dreifuss muscular dystrophy. *J. Cell Biol.* **184**, 31-44.
- Miller, T. M., Kim, S. H., Yamanaka, K., Hester, M., Umapathi, P., Arnson, H., Rizo, L., Mendell, J. R., Gage, F. H., Cleveland, D. W. et al.** (2006). Gene transfer demonstrates that muscle is not a primary target for non-cell-autonomous toxicity in familial amyotrophic lateral sclerosis. *Proc. Natl. Acad. Sci. USA* **103**, 19546-19551.
- Nicot, A. S. and Laporte, J.** (2008). Endosomal phosphoinositides and human diseases. *Traffic* **9**, 1240-1249.
- Nicot, A. S., Toussaint, A., Tosch, V., Kretz, C., Wallgren-Pettersson, C., Iwarsson, E., Kingston, H., Garnier, J. M., Biancalana, V., Oldfors, A. et al.** (2007). Mutations in amphiphysin 2 (BIN1) disrupt interaction with dynamin 2 and cause autosomal recessive centronuclear myopathy. *Nat. Genet.* **39**, 1134-1139.
- Pierson, C. R., Tomczak, K., Agrawal, P., Moghadaszadeh, B. and Beggs, A. H.** (2005). X-linked myotubular and centronuclear myopathies. *J. Neuropathol. Exp. Neurol.* **64**, 555-564.
- Pierson, C. R., Agrawal, P. B., Blasko, J. and Beggs, A. H.** (2007). Myofiber size correlates with MTM1 mutation type and outcome in X-linked myotubular myopathy. *Neuromuscul. Disord.* **17**, 562-568.
- Pierson, C. R., Dulin-Smith, A., Durban, A., Marshall, M., Marshall, J., Snyder, A., Naier, A., Gladman, J., Chandler, D., Lawlor, M. W. et al.** (2012). Modeling the human MTM1p.R69C mutation in murine Mtm1 results in exon 4 skipping and a less severe myotubular myopathy phenotype. *Hum. Mol. Genet.* **21**, 811-825.
- Rando, T. A. and Blau, H. M.** (1994). Primary mouse myoblast purification, characterization, and transplantation for cell-mediated gene therapy. *J. Cell Biol.* **125**, 1275-1287.
- Rimer, M.** (2007). Neuregulins at the neuromuscular synapse: past, present, and future. *J. Neurosci. Res.* **85**, 1827-1833.
- Robb, S. A., Sewry, C. A., Dowling, J. J., Feng, L., Cullup, T., Lillis, S., Abbs, S., Lees, M. M., Laporte, J., Manzur, A. Y. et al.** (2011). Impaired neuromuscular transmission and response to acetylcholinesterase inhibitors in centronuclear myopathies. *Neuromuscul. Disord.* **21**, 379-386.
- Robinson, F. L. and Dixon, J. E.** (2006). Myotubularin phosphatases: policing 3-phosphoinositides. *Trends Cell Biol.* **16**, 403-412.
- Skeie, G. O., Apostolski, S., Evoli, A., Gilhus, N. E., Illa, I., Harms, L., Hilton-Jones, D., Melms, A., Verschuuren, J. and Horge, H. W.** (2010). Guidelines for treatment of autoimmune neuromuscular transmission disorders. *Eur. J. Neurol.* **17**, 893-902.
- Toussaint, A., Cowling, B. S., Hnia, K., Mohr, M., Oldfors, A., Schwab, Y., Yis, U., Maisonobe, T., Stojkovic, T., Wallgren-Pettersson, C. et al.** (2011). Defects in amphiphysin 2 (BIN1) and triads in several forms of centronuclear myopathies. *Acta Neuropathol.* **121**, 253-266.
- Wilmshurst, J. M., Lillis, S., Zhou, H., Pillay, K., Henderson, H., Kress, W., Muller, C. R., Ndondo, A., Cloke, V., Cullup, T. et al.** (2010). RYR1 mutations are a common cause of congenital myopathies with central nuclei. *Ann. Neurol.* **68**, 717-726.
- Wirtz, P. W., Titulaer, M. J., Gerven, J. M. and Verschuuren, J. J.** (2010). 3,4-diaminopyridine for the treatment of Lambert-Eaton myasthenic syndrome. *Expert Rev. Clin. Immunol.* **6**, 867-874.
- Won, S., Si, J., Colledge, M., Ravichandran, K. S., Froehner, S. C. and Mei, L.** (1999). Neuregulin-increased expression of acetylcholine receptor epsilon-subunit gene requires ErbB interaction with Shc. *J. Neurochem.* **73**, 2358-2368.
- Wu, B., Goluszko, E. and Christadoss, P.** (2001). Experimental autoimmune myasthenia gravis in the mouse. *Curr. Protoc. Immunol.* **Chapter 15**, Unit 15.18.
- Yang, X. L., Huang, Y. Z., Xiong, W. C. and Mei, L.** (2005). Neuregulin-induced expression of the acetylcholine receptor requires endocytosis of ErbB receptors. *Mol. Cell Neurosci.* **28**, 335-346.